pubs.acs.org/acschemicalbiology

Articles

Receptor–Ligand Kinetics Influence the Mechanism of Action of Covalently Linked TLR Ligands

Flora W. Kimani,[§] Jainu Ajit,[§] Alexander Galluppi, Saikat Manna, William J. Howitz, Sophia Tang, and Aaron P. Esser-Kahn*

Cite This: *ACS Chem. Biol.* 2021, 16, 380–388

Read Online

ACCESS | Metrics & More | Article Recommendations | Supporting Information

ABSTRACT: We report a mechanistic study comparing the immune activation of conjugated Toll-like receptor (TLR) agonists and their unlinked mixtures. Herein, we synthesized a set of six linked dual agonists with different ligands, molecular structures, receptor locations, and biophysical characteristics. With these dimers, we ran a series of *in vitro* cell-based assays, comparing initial and overall NF-κB (nuclear factor kappa-light-chain-enhancer of activated B cells) activation, cytokine expression profiles, as well as time-resolved TNF-α (Tumor Necrosis Factor alpha) expression. We show that initial activation kinetics, ligand specificity, and the dose of the agonist influence the activity of these linked TLR systems. These results can help improve vaccine design by showing how linked TLR agonists can improve their potency with the appropriate selection of key criteria.

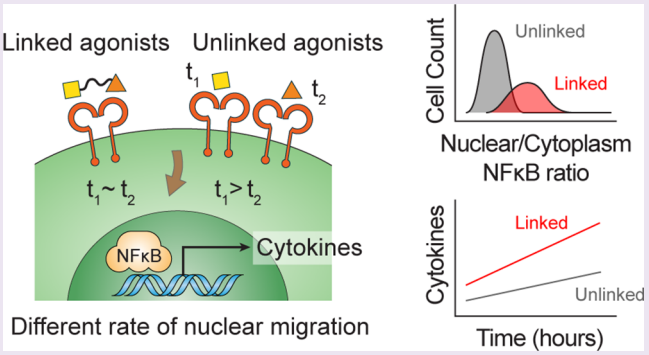

Whole-cell vaccines produce potent and prolonged immune responses against pathogens. The efficacy of whole vaccines is due to the simultaneous presentation of multiple pathogen-associated molecular patterns (PAMPs) to innate immune cells, often leading to a robust response and overall protection.[1,2] Innate immune cells are activated by the recognition and binding of specific PAMPs to receptors such as Toll-like receptors (TLRs).[3] This causes a complex signaling cascade that results in the production of inflammatory cytokines, chemokines, and costimulatory molecules, which then modulate the magnitude and duration of antigen-specific adaptive responses.[4−6] In previous work, we have shown that linked combinations of TLR agonists can serve as a unique alternative to the traditional whole-cell vaccines through spatially constrained multi-TLR presentation and activation. Additionally, such constructs are immunomodulatory, allowing for fine-tuned responses against pathogens of interest.[7−9] Multi-TLR agonists are therefore promising candidates for application as immunostimulants (adjuvants) in subunit vaccines and are currently included in several preclinical trials.[10,11] We also found that covalently linked agonists induce synergistic responses by increasing inflammatory cytokines and promoting a T_H1-biased response compared to the unlinked agonist mixtures. We observed spatial inductions that change the cytokine and antibody profile as well as epitope affinity.[7,12,13] Others have shown that the immune cell response to dual stimulation by a mixture of unlinked agonists and cytokines leads to distinct ligand and dose-dependent NF-κB dynamics.[14,15] Simultaneous activation of TLR 2 and 4 in a cell population using a mixture of Pam_3CSK_4 and LPS resulted in each cell's NF-κB dynamics resembling the response to one or the other ligand and not a combination of both.[14] In contrast, a mixture of TNF-α and LPS led to a combinatory response of NF-κB dynamics.[15] These results taken together suggest that cells have a complex system of integrating and processing multi-TLR signals that may be dependent on upstream events in the NF-κB activation pathway.

Most mechanistic studies of synergistic induction by multiple stimuli have been conducted using mixtures of agonists or cytokines. In our continued efforts to move toward rational development of immune agonists that mimic their spatial distribution in a pathogen, we sought to investigate the mechanism of action of spatially controlled, covalently linked dual TLR agonists. To achieve this, we synthesized a small library of six combinations of linked agonists—varying the size of the agonist, signaling adaptor involved, and the location of the TLR. With these six dimers, we ran a series of *in vitro* experiments on murine macrophages to define the structural and molecular mechanisms that influence immune responses of linked dual TLR ligands.

Received: December 1, 2020
Accepted: January 26, 2021
Published: February 1, 2021

https://dx.doi.org/10.1021/acschembio.0c00924
ACS Chem. Biol. 2021, 16, 380–388

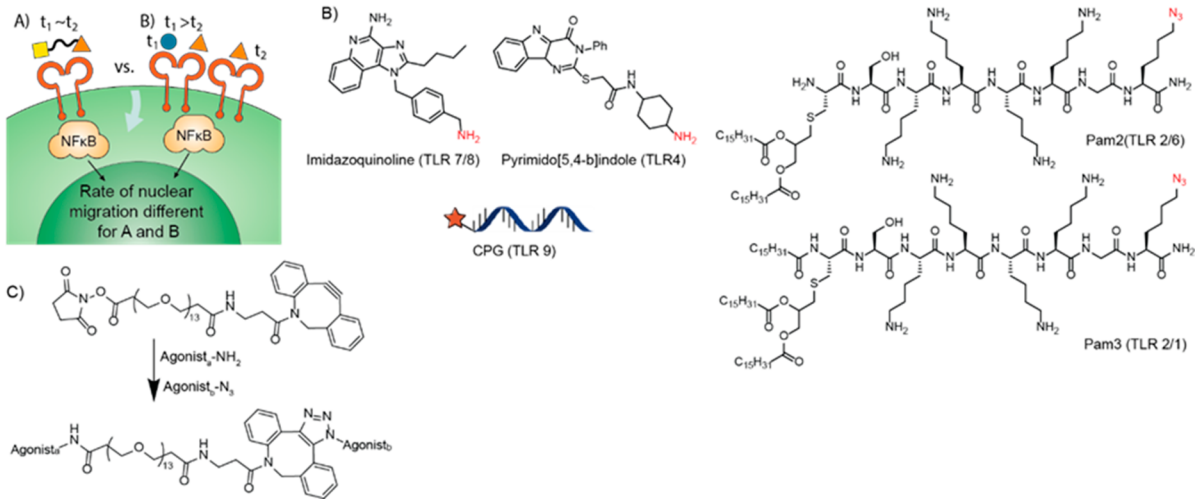

Figure 1. Comparing the mechanism of NF-κB migration and subsequent immune response after activation with linked agonist and unlinked agonist mixture. (B) Molecular structures of agonist selected in this study. (C) Covalent site-specific linking strategy for synthesis of linked TLR agonist dimers.

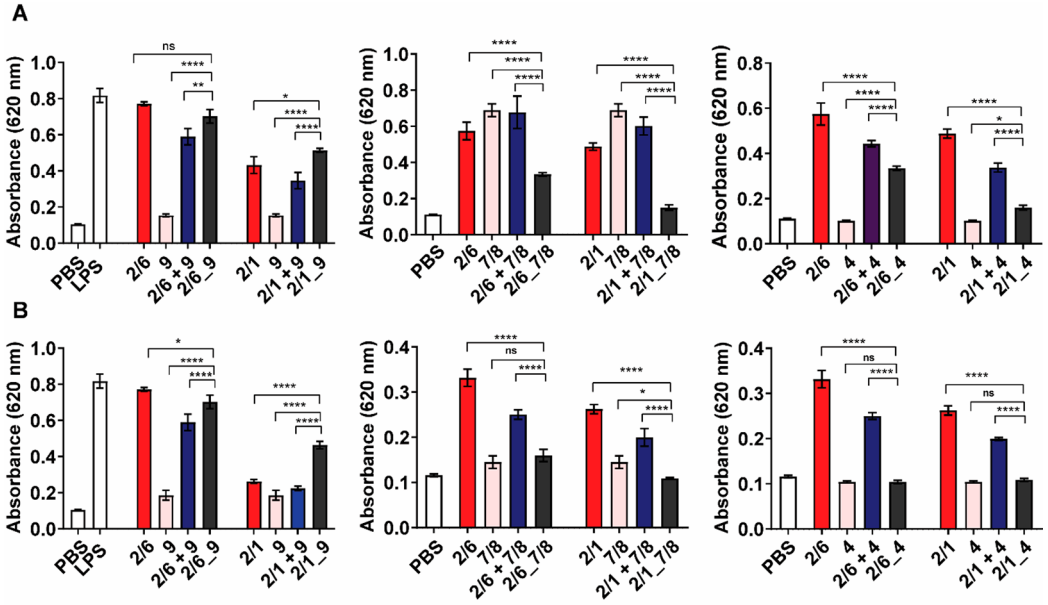

Figure 2. Immune activation of Pam_2CSK_4 (2/6), Pam_3CSK_4 (2/1), CpG_1826 (9), indole (4), and imidazoquinoline (7/8), corresponding equimolar mixtures and linked agonists measured by RAW-Blue activation via NF-κB stimulation after 24 h of incubation at 37 °C. (A) 50 nM, (B) 10 nM. Samples run in triplicate. Statistical significance is between the single, unlinked mixtures vs linked agonists, compared by the one-way ANOVA. *$p \leq 0.05$, ****$p \leq 0.0001$

To examine the immune responses of the dual agonists, we employed an NF-κB reporter cell line and profiled the responses as (1) unaltered, (2) additive, or (3) subtractive. We correlated these results with time course analysis on reporter cell lines and secretion of TNF-α. The results indicated that the synergistic interactions from linked agonists were dose-as well as ligand-dependent. These differences correlate with differences in early NF-κB activation dynamics resulting in distinct profile patterns. The data suggest that the kinetics within the first 30 min of ligand−receptor processing as well as ligand specificity play a pivotal role in the mechanism of linked agonist activation and provide insight into how immune cells process exposure to dual stimuli in a linked system.

RESULTS

Synthesis of Covalently Linked Agonists. TLRs recognize a varied set of PAMPs and can be further classified based on the ligands that activate the TLRs; TLR 1, 2, and 6 recognize lipids; TLR 3, 7, 8, and 9 recognize nucleic acids; and TLR 4 recognizes diverse structural elements.[3] To investigate the mechanism of action of the linked TLR agonists, we needed to synthesize a set of molecules sufficient to test (1) molecular variation, (2) receptor location variation, and (3) differences in biophysical characteristics of the ligand. While the TLR system is limited in the available ligands, we selected five molecules of varying size and receptor identity to form six combinations. The six combinations were made up of synthetic lipopeptides Pam_2CSK_4 (TLR 2/6) and Pam_3CSK_4 (TLR 2/1),[16−18] synthetic oligonucleotides CPG_ODN 1826

https://dx.doi.org/10.1021/acschembio.0c00924
ACS Chem. Biol. 2021, 16, 380−388

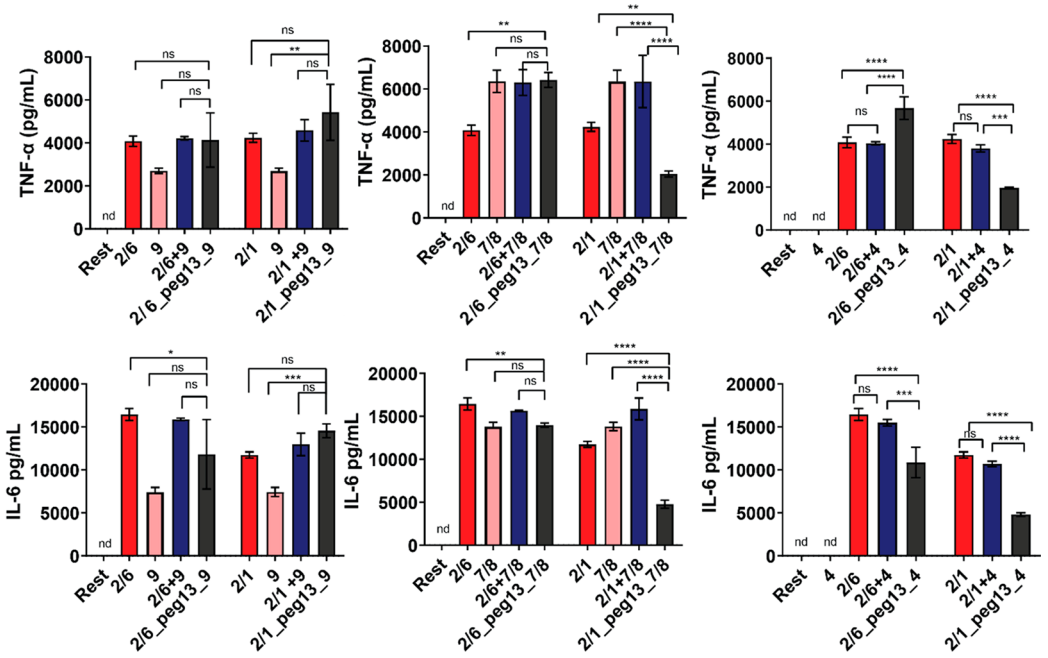

Figure 3. *In vitro* cytokine production from BMDC cells measured by cytokine bead array assay. Cells were incubated with 25 nM of Pam_2CSK_4 (2/6), Pam_3CSK_4 (2/1), CpG_1826 (9), indole (4), and imidazoquinoline (7/8); corresponding equimolar mixtures; and linked agonists for 24 h at 37 °C and 5% CO_2. Samples run in triplicate. Statistical significance is between the single, unlinked mixtures vs linked agonists, compared by the one-way ANOVA. *$p \leq 0.05$, ****$p \leq 0.0001$

(TLR 9),[19] pyrimido[5,4-*b*]indole (TLR 4),[20,21] and imidazoquinoline (TLR 7/8).[22] To covalently link the agonists, we synthesized derivatives with orthogonal conjugatable handles and used a heterotelechelic polyethylene glycol (PEG) discrete linker. We installed azide groups on the lipopeptides and used amine-derivatized indole[20] and imidazoquinoline[22] and CPG for conjugation. With these agonists we made the following pairs: 2/6_peg13_4, 2/6_peg13_7/8, 2/1_peg13_4, 2/1_peg13_7/8, 2/6_peg13_9, and 2/1_peg13_9 (Figure 1). On the basis of previous work done by us and others,[23] we did not synthesize homodimers (e.g., 4_4 or 9_9) as we were interested in inducing dual TLR stimuli. Similarly, 2/6 and 2/1 both target TLR2-containing receptor complexes rendering dimers of the two as possible antagonists of one or both pathways. Additionally, 7/8_9, dimer targeting endosomal receptors, never showed altered responses in our hands, and we have not reported on these molecules further. These rules left us with these six combinations to examine. The synthesized dimers were purified by chromatographic techniques and spectroscopically characterized. Synthetic lipopeptides have been shown to self-assemble into micelle structures when studied at a concentration of 0.5 wt %.[24] In this mechanistic study, we sought to rule out self-assembly of the dimers and the influence of secondary structure to immune response. We characterized the dimers by dynamic light scattering in pH 7.4 PBS at experimentally relevant concentrations to investigate possible particle formation and aggregation. At concentrations of 250 nM and above, we observed that the lipopeptide−small molecule dimers formed larger particles than those of the parent lipopeptides (SI Figure 4). 2/1_peg13_4 and 2/1_peg13_7/8 dimers showed evidence of aggregation with no uniform distribution of particles. However, we did not observe particle formation by DLS at the lower concentrations that we used for *in vitro* analyses.

NF-κB Activity of TLR Dimers. Initially, we sought to ascertain the differences in activity between these compounds. TLR activation by ligands or agonists activates MyD88 and TRIF pathways where the downstream effect is the activation of transcription factors NF-κB and AP-1 (Activator Protein 1).[25] Using the RAW 264.7 macrophage reporter cell line, RAW-Blue, we profiled the overall transcriptional activity of the linked agonists by measuring the level of secreted embryonic alkaline phosphatase (SEAP) induced by both NF-κB and AP-1. The lipopeptide-CPG dimers, 2/1_peg13_9 and 2/6_peg13_9, showed significantly higher activity than the corresponding equimolar agonist mixtures (Figure 2). 2/6_peg13_9 was slightly higher compared to the agonist mixtures and the monomers, while 2/1_peg13_9 showed an additive response at 10 nM concentration. Surprisingly, the small molecule derived dimers of Pam_2CSK_4, 2/6_peg13_4 and 2/6_peg13_7/8 2/1_peg13_4 and 2/1_peg13_7/8, showed a subtractive response when compared to the individual and unlinked mixture of agonists. Reduction in activity for conjugated small molecule agonists such as the indole and the imidazoquinoline has been reported and could be attributed to a disruption in the receptor−agonist interactions.[8] In some cases, either the activity is restored due to synergistic effects after conjugation or the dimer retains the activity of the more potent monomer. In this case, the small molecules conjugated onto the lipopeptide agonists did not increase the cellular response. However, the decrease in activity was not expected, indicating a possible molecular change in the cellular immune response. The set of six dimers were representative of additive, subtractive, and unaltered effects, which made it an ideal toolset to study.

Comparing Cytokine Secretion Profiles of Linked and Unlinked Agonists. After analysis of overall immune activation using RAW-Blue assay, we compared the cytokine profile of cells treated with linked and unlinked equimolar

https://dx.doi.org/10.1021/acschembio.0c00924
ACS Chem. Biol. 2021, 16, 380−388

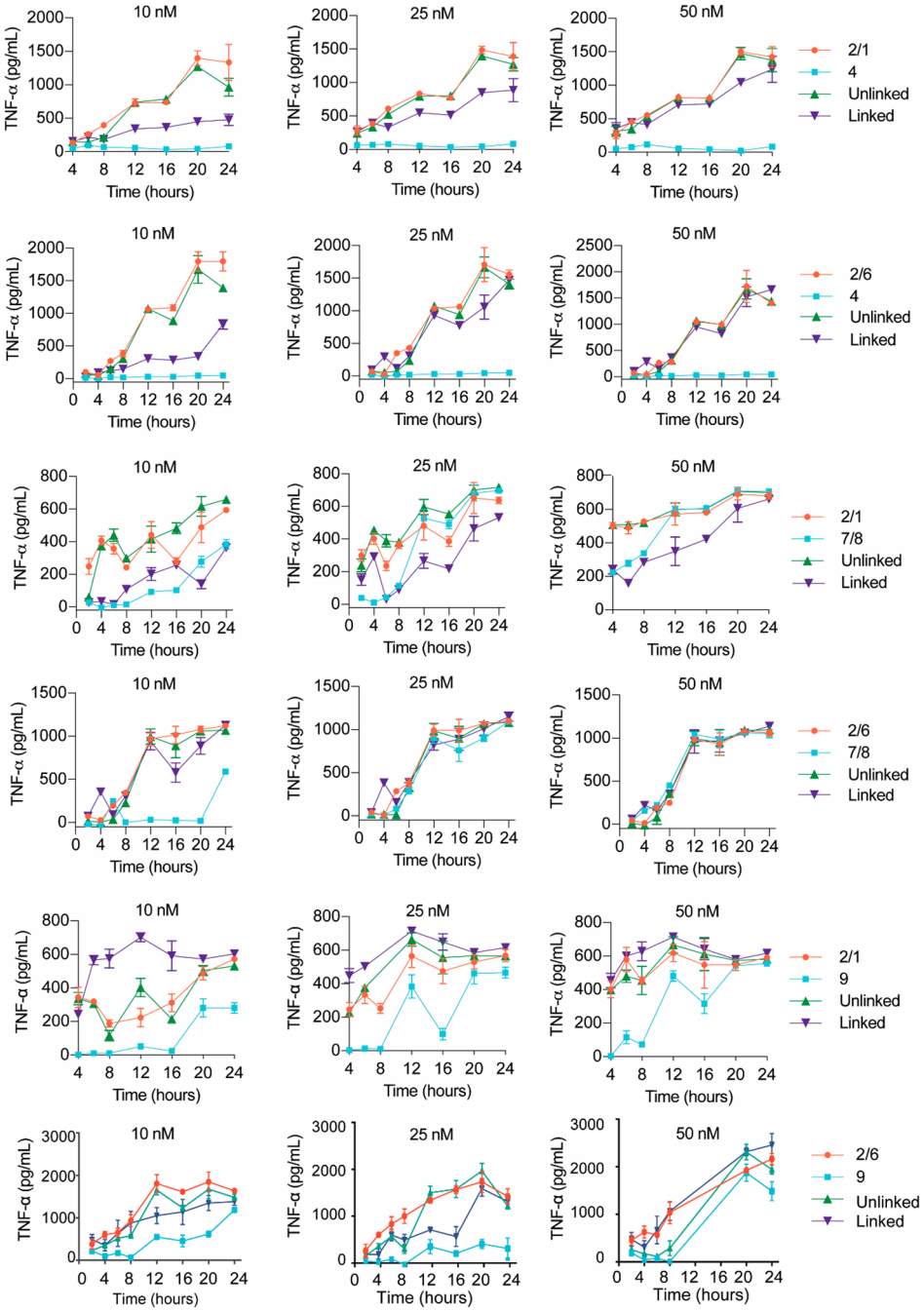

Figure 4. Kinetic profiling of cytokine TNF-α secretion. RAW macrophages were incubated with Pam_2CSK_4 (2/6), Pam_3CSK_4 (2/1), CpG_1826 (9), indole (4), and imidazoquinoline (7/8); corresponding equimolar mixtures; and linked agonists at 10, 25, and 50 nM concentrations. Secreted TNF-α in the supernatant was measured at defined time intervals for 24 h. The supernatant was incubated with the HEK-Blue TNF-α reporter cell line for 20 to 24 h and quantified using TNF-α standards by measuring secreted SEAP levels.

heterodimer agonists. Equimolar mixtures of agonists and ligands resulted in either synergistic or inhibitory cytokine responses. The downstream effects are governed by the interaction of the MyD88 and TRIF pathways. Upon recognition of PAMPs, TLRs initiate downstream signaling with the help of adaptor proteins, mainly MyD88 and TIR-domain-containing adapter-inducing interferon-β (TRIF). While all TLRs except TLR 3 activate MyD88, TRIF is only activated by TLR 3 and 4. MyD88 signaling leads to the activation of NF-κB, thereby producing pro-inflammatory cytokines such as IL-6 and TNF-α. Signaling through the TRIF pathway results in the production of inflammatory cytokines and type 1 interferons. TLR4 activates both MyD88 and TRIF pathways.[5] Inhibitory responses are caused by tolerance induced by sequential activation of multiple pathways.[26−28] By conjugating the agonists, we had more spatial and temporal control on the simultaneous activation of dual TLR receptors on a single cell. We incubated bone marrow-derived dendritic cells (BMDCs) with 25 nM linked agonists and the corresponding equimolar single agonist. We measured the secreted cytokines after 24 h using an inflammatory-panel cytokine-bead-array assay for IL-6, IL-10, MCP-1, IFN-γ, TNF-α, and IL-12p70. We detected measurable levels of TNF-α, MCP-1, and IL-6 levels at this

https://dx.doi.org/10.1021/acschembio.0c00924
ACS Chem. Biol. 2021, 16, 380−388

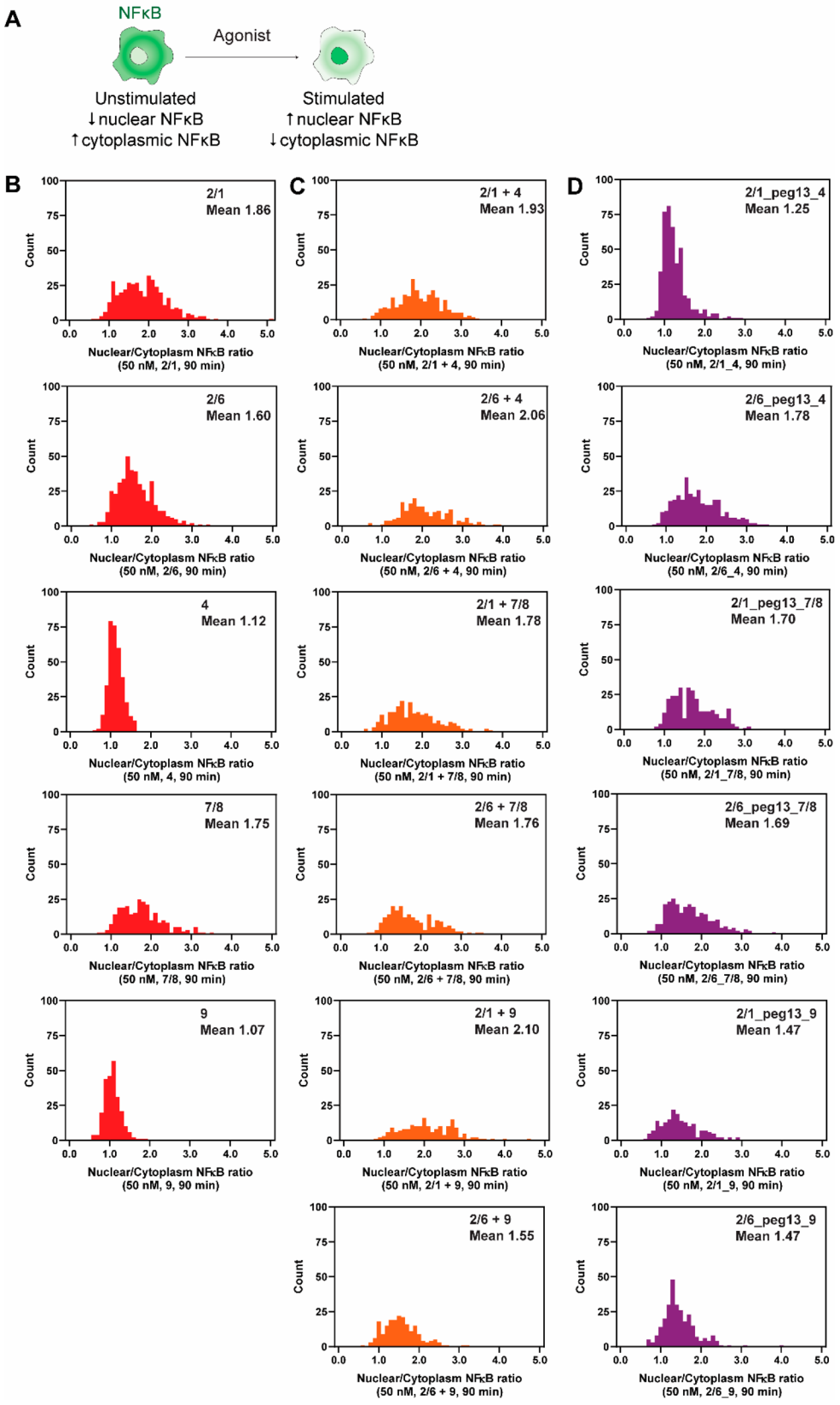

Figure 5. Single-cell analysis NF-κB migration studies. (A) GFP-NF-κB migration from the cytoplasm to the nucleus. RAW-G9 cells containing NF-κB-GFP are imaged, and the kinetics of NF-κB migration into the nucleus are quantified after 90 min of stimulation with 50 nM. (B) Pam_2CSK_4 (2/6), Pam_3CSK_4 (2/1), CPG (9), indole (4), and imidazoquinoline (7/8). (C) Corresponding equimolar mixtures and (D) linked agonists. Each image contains a distribution of the ratios for all cells in the field of view for multiple images. Mean values were calculated from all available data.

https://dx.doi.org/10.1021/acschembio.0c00924
ACS Chem. Biol. 2021, 16, 380−388

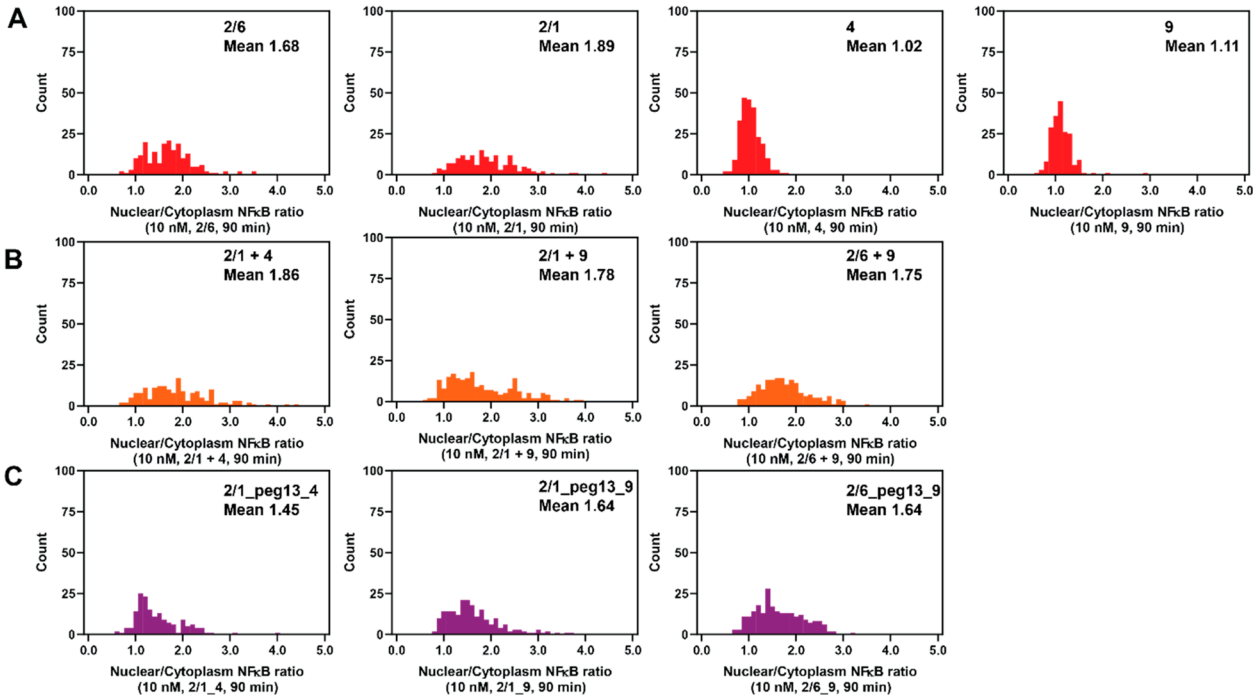

Figure 6. Effect of dose on NF-κB migration. RAW-G9 cells containing NF-κB-GFP are imaged, and the kinetics of NF-κB migration into the nucleus are quantified after 90 min of stimulation with 10 nM (A) Pam_2CSK_4 (2/6), Pam_3CSK_4 (2/1), CPG (9), and indole (4). (B) Corresponding equimolar mixtures and (C) linked agonists. Each image contains a distribution of the ratios for all cells in the field of view for multiple images. Mean values were calculated from all available data.

concentration. We observed no significant differences in cytokine production between the lipopeptide−CPG dimers and the corresponding monomers and unlinked mixtures. Most lipopeptide derived indole dimers showed lower levels of TNF-α, IL-6, and MCP-1—except 2/6_peg13_4, which had higher levels of TNF-α (Figure 3). This cytokine secretion profile correlated results from the RAW-Blue assay, indicating that for these dimers, the level of activation of NF-κB was linked to the amount of cytokine secreted. On the other hand, we did not observe any synergistic or additive secretion of cytokines in cells treated with the 2/1_peg13_9 dimer, which had shown higher immune response in the RAW-Blue assay. In addition, the 2/6_peg13_7/8 dimer induced similar cytokine secretion levels in contrast to the lower immune activity as shown by the RAW-Blue assay at the same concentration.

Effect of Dose on TNF-α Secretion over Time. After observing the differences in cytokines, we became curious as to why these differences appeared to contrast so much between different compounds and different agonist sets. In these experiments, we noted that, while TNF-α levels appeared similar after 24 h, at earlier time points there were distinct differences, implying that kinetics of synergistic interactions are related to early time points. We decided to explore these kinetic differences further, as they seemed to show a potential explanation for clear distinctions between the agonists. Investigating TNF-α secretion could explain the differences observed in the other cytokines and provide a standard basis for comparison, as most agonist sets resulted in similar levels at 24 h. In previous reports, we have also observed that lowering agonist concentration can sometimes alter the synergistic response, so we conducted our kinetic screen with varying concentrations. Using RAW 264.7 macrophages, we measured the secretion of TNF-α from 0 to 24 h at 2 and 4 h intervals after stimulating the cells with agonists at concentrations of 10, 25, and 50 nM. We observed dose-and time-dependent activity for the different agonist combinations. At lower concentrations (10 nM), treatment with 2/1_peg13_4, 2/6_peg13_4, and 2/1_peg13_7/8 dimers consistently produced lower cytokine secretion over 24 h. As the dose was increased, these dimers activated RAW 264.7 cells at comparable levels to those of the unlinked equimolar mixtures (Figure 4). These data suggest that activation of TLRs was modulated by the rate of receptor−agonist interactions for these dimers, which increased as the dimer concentration increased. However, for the 2/1_peg13_9 dimer, we observed a significant increase in TNF-α secretion at lower concentrations, but this effect was not observed at higher concentrations. This correlated with the overall immune activity data measured by RAW-Blue assay (Figure 2), suggesting that a synergistic activation involving these specific 2/1 and 9 agonists is facilitated by conjugation.

NF-κB Translocation Kinetics. Upon observing the differences in cytokine production that did not uniformly correlate with the overall immune activity measured by RAW-Blue assay 24 h after activation, we hypothesized that initial transcription kinetics would give insight into the differences in activity. This hypothesis is based on mounting evidence that NF-κB activation and translocation from cytoplasm to the nucleus is a rapid response to TLR activation and the first step toward transcription of immune genes.[29] We expected that a synergistic response would correlate to a higher rate of transcription and, conversely, that an inhibitory response would correlate to a lower rate of transcription. Using an engineered RAW 264.7 cell line with a stably expressed GFP-tagged fusion of the RelA NF-κB protein, we quantified and compared the rate of NF-κB translocation of the linked agonists and unlinked mixtures.[30] After treating the cells with the linked agonists and the corresponding single and unlinked mixtures, we used confocal microscopy to track GFP-tagged

https://dx.doi.org/10.1021/acschembio.0c00924
ACS Chem. Biol. 2021, 16, 380−388

NF-κB translocation from cytoplasm to the nucleus. A nuclear stain allowed us to calculate the ratio of nuclear to cytoplasmic NF-κB in each cell using CellProfiler. Using this technique, we resolved single-cell-level differences in NF-κB response dynamics. Comparing distributions of single-cell activation, we observed distinct patterns of activation of the cells when treated with the dimers, equimolar mixtures, or single agonists. The activation profiles of most of the unlinked mixtures resembled that of the monomers. Most of the dimers seemed to follow this trend and resemble the unlinked mixtures and the monomers in the activation profiles. In contrast the 2/1_peg13_4 dimer profile matched the TLR 4 agonist with the unlinked mixture resembling the TLR 2/1 agonist (Figure 5). Interestingly, these data correlate closely with the difference we had observed in the RAW-Blue assay (Figure 2) where we saw significant differences in activity for the indole (TLR 4) activating dimers. These distinct profile patterns indicate that the linked agonists' activation of NFκB is determined by specific ligand interactions.

When we investigated the effect of dose on the NF-κB activation profiles, we observed a change in the activation profile of the 2/1_peg13_4 dimer. At this lower concentration (10 nM), the dimer activated more cells to a >2 nuclear/cytoplasm ratio. The profile also seemed to resemble the activation profile of the lipopeptide, and the mixture of agonists (2/1 and 2/1 + 4). However, the lipopeptide−CPG dimers had a similar NF-κB activation profile similar to that of the lipopeptides and the agonist mixtures at both concentrations (Figure 6).

DISCUSSION

Linked TLR agonists elicit unique responses in both *in vitro* and *in vivo* systems. Understanding how these multiactivating systems works is key in the rational development of vaccine adjuvants. Combinatory responses to multiple stimuli by unlinked agonist mixtures is correlated to synergistic immune responses and distinct NF-κB activation profiles. Previous work has shown that cellular integration and processing of these multiple stimuli is specific to the type of NF-κB activating stimuli and processing capacity.[14,15] Our study on the mechanism of activation of linked dual TLR agonists suggests that ligand−receptor interactions influence initial transcriptional kinetics and thus downstream cytokine secretion profiles. The immune response is also dictated by specific single ligand interactions which can be attributed to the physical characteristics of the dimer constituents, the potency of the agonist pair, or the pathway (MyD88 and TRIF) that is activated by the agonist pair.

Overall NF-κB activity measured by RAW 264.7 cells showed significant differences in immune response when comparing between linked and unlinked agonists. These differences in activity were dose-and agonist-dependent with unaltered, additive, and inhibitory outcomes. Synthetic lipopeptides Pam_3CSK_4 and Pam_2CSK_4 both stimulate cell surface, membrane-bound TLR2 complexes. However, the dimers derived by conjugating these two agonists to small-molecule agonists—indole (TLR4) and imidazoquinoline (TLR7/8)—had different immune activity and cytokine secretion profiles. The dimers showed inhibitory NF-κB immune activity with lower downstream cytokine secretion compared to treatment with the lipopeptides and agonist mixtures. The lipopeptide−CPG dimers showed an increase in immune activity that was more pronounced at lower concentrations.

By evaluating single-cell NF-κB dynamics, we observed that 2/1_peg13_4 had a similar profile as the cells stimulated with indole (TLR 4), suggesting that this dimer preferentially activates through TLR 4. The low potency of the TLR4 activating indole could explain the decrease in the immune activity of this dimer especially if the dimer preferentially activates through the TLR 4 receptor. This agonist biasing effect was not observed with the 2/1_peg13_7/8, 2/6_peg13_4, and the 2/6_peg13_7/8, which had a similar profile as the corresponding unlinked mixture and the single agonists. Additionally, the time course of TNF-α cytokine secretion over time further illustrates the dose and agonist specificity of the linked agonists. Ligand−receptor interactions depend on the dose of the agonist with the high immune response being attributed to increased interactions. In the TNF-α secretion data set, we observe that an increase in the dose of 2/1_peg13_7/8 and 2/1_peg13_4 dimers from 10 nM to 50 nM led to similar levels of cytokine production as the unlinked agonist and the corresponding mixtures. However, in the case of 2/1_peg13_9, we observe synergy in the overall immune response as well as in TNF-α secretion in lower concentrations but not at higher concentrations, indicating that for this dimer the synergistic interaction is derived from the altered kinetics of NF-κB signaling. While we have not definitively concluded what physical phenomenon results in the altered kinetics, by contrasting TLR 2/1and TLR 2/6 systems, we can conjecture that the difference may stem either from specific receptor pairings enhanced by linkage or by strong lipid interactions of the tripalmitoylation of the TLR 2/1 agonist.

In this study, we show that the activity of dual linked agonists is both ligand- and dose-dependent. By observing the initial kinetics of activation, we observed distinct NF-κB dynamics that can be attributed to how the immune cells integrate and process two activation signals, which further informs the downstream immune response. Using this set of dimers, we show ligand-dependent immune response with synergy being induced with only specific sets of dimers. We also observe a dependence of dose on the magnitude of the immune response, which indicates that kinetics of receptor activation by the ligands play a role in the mechanism of activation in linked systems.

ASSOCIATED CONTENT

Supporting Information

The Supporting Information is available free of charge at https://pubs.acs.org/doi/10.1021/acschembio.0c00924.

Synthesis of conjugated agonists and heterodimers, characterization, and additional cell assay data (PDF)

AUTHOR INFORMATION

Corresponding Author

Aaron P. Esser-Kahn − *Pritzker School of Molecular Engineering, University of Chicago, Chicago, Illinois 60637, United States;* orcid.org/0000-0003-1273-0951; Email: aesserkahn@uchicago.edu

Authors

Flora W. Kimani − *Pritzker School of Molecular Engineering, University of Chicago, Chicago, Illinois 60637, United States*

https://dx.doi.org/10.1021/acschembio.0c00924
ACS Chem. Biol. 2021, 16, 380−388

Jainu Ajit − *Pritzker School of Molecular Engineering, University of Chicago, Chicago, Illinois 60637, United States*
Alexander Galluppi − *Pritzker School of Molecular Engineering, University of Chicago, Chicago, Illinois 60637, United States*
Saikat Manna − *Pritzker School of Molecular Engineering, University of Chicago, Chicago, Illinois 60637, United States;* orcid.org/0000-0002-0809-5695
William J. Howitz − *Department of Chemistry, University of California, Irvine, Irvine, California 92697-2025, United States;* orcid.org/0000-0001-6323-7126
Sophia Tang − *Pritzker School of Molecular Engineering, University of Chicago, Chicago, Illinois 60637, United States*

Complete contact information is available at: https://pubs.acs.org/10.1021/acschembio.0c00924

Author Contributions

[§]These authors contributed equally.

Funding

The authors acknowledge the financial support provided by National Institutes of Health (7U01AI124286-03)

Notes

The authors declare no competing financial interest.

■ ACKNOWLEDGMENTS

We thank the core facilities at University of Chicago for assistance with materials characterization. We also thank the Integrated Light Microscopy Core for assistance with imaging experiments.

■ REFERENCES

(1) Pulendran, B., and Ahmed, R. (2011) Immunological mechanisms of vaccination. *Nat. Immunol. 12*, 509−517.
(2) Ahmed, R., and Pulendran, B. (2011) Learning vaccinology from viral infections. *J. Exp. Med. 208*, 2347−2349.
(3) Akira, S., Uematsu, S., and Takeuchi, O. (2006) Pathogen recognition and innate immunity. *Cell 124*, 783−801.
(4) Parker, L. C., Prince, L. R., and Sabroe, I. (2007) Translational mini-review series on Toll-like receptors: Networks regulated by Toll-like receptors mediate innate and adaptive immunity. *Clin. Exp. Immunol. 147*, 199−207.
(5) Kawasaki, T., and Kawai, T. (2014) Toll-like receptor signaling pathways. *Front. Immunol. 5*, 461.
(6) Tipping, P. G. (2006) Toll-like receptors: The interface between innate and adaptive immunity. *J. Am. Soc. Nephrol. 17*, 1769−1771.
(7) Tom, J. K., Dotsey, E. Y., Wong, H. Y., Stutts, L., Moore, T., Davies, D. H., Felgner, P. L., and Esser-Kahn, A. P. (2015) Modulation of innate immune responses via covalently linked TLR agonists. *ACS Cent. Sci. 1*, 439−448.
(8) Albin, T. J., Tom, J. K., Manna, S., Gilkes, A. P., Stetkevich, S. A., Katz, B. B., Supnet, M., Felgner, J., Jain, A., Nakajima, R., Jasinskas, A., Zlotnik, A., Pearlman, E., Davies, D. H., Felgner, P. L., Burkhardt, A. M., and Esser-Kahn, A. P. (2019) Linked Toll-Like Receptor Triagonists Stimulate Distinct, Combination-Dependent Innate Immune Responses. *ACS Cent. Sci. 5*, 1137−1145.
(9) Gilkes, A. P., Albin, T. J., Manna, S., Supnet, M., Ruiz, S., Tom, J., Badten, A. J., Jain, A., Nakajima, R., Felgner, J., Davies, D. H., Stetkevich, S. A., Zlotnik, A., Pearlman, E., Nalca, A., Felgner, P. L., Esser-Kahn, A. P., and Burkhardt, A. M. (2020) Tuning Subunit Vaccines with Novel TLR Triagonist Adjuvants to Generate Protective Immune Responses against Coxiella burnetii. *J. Immunol. 204*, 611−621.
(10) Madan-Lala, R., Pradhan, P., and Roy, K. (2017) Combinatorial Delivery of Dual and Triple TLR Agonists via Polymeric Pathogen-like Particles Synergistically Enhances Innate and Adaptive Immune Responses. *Sci. Rep. 7*, 2530.
(11) Orr, M. T., Beebe, E. A., Hudson, T. E., Moon, J. J., Fox, C. B., Reed, S. G., and Coler, R. N. (2014) A dual TLR agonist adjuvant enhances the immunogenicity and protective efficacy of the tuberculosis vaccine antigen ID93. *PLoS One 9*, No. e83884.
(12) Mancini, R. J., Tom, J. K., and Esser-Kahn, A. P. (2014) Covalently coupled immunostimulant heterodimers. *Angew. Chem., Int. Ed. 53*, 189−92.
(13) Ryu, K. A., Slowinska, K., Moore, T., and Esser-Kahn, A. (2016) Immune Response Modulation of Conjugated Agonists with Changing Linker Length. *ACS Chem. Biol. 11*, 3347−3352.
(14) Kellogg, R. A., Tian, C., Etzrodt, M., and Tay, S. (2017) Cellular Decision Making by Non-Integrative Processing of TLR Inputs. *Cell Rep. 19*, 125−135.
(15) Gutschow, M. V., Mason, J. C., Lane, K. M., Maayan, I., Hughey, J. J., Bajar, B. T., Amatya, D. N., Valle, S. D., and Covert, M. W. (2019) Combinatorial processing of bacterial and host-derived innate immune stimuli at the single-cell level. *Mol. Biol. Cell 30*, 282−292.
(16) Takeuchi, O., Kawai, T., Mühlradt, P. F., Morr, M., Radolf, J. D., Zychlinsky, A., Takeda, K., and Akira, S. (2001) Discrimination of bacterial lipoproteins by Toll-like receptor 6. *Int. Immunol. 13*, 933−940.
(17) Buwitt-Beckmann, U., Heine, H., Wiesmüller, K. H., Jung, G., Brock, R., Akira, S., and Ulmer, A. J. (2005) Toll-like receptor 6-independent signaling by diacylated lipopeptides. *Eur. J. Immunol. 35*, 282−289.
(18) Aliprantis, A. O., Yang, R. B., Mark, M. R., Suggett, S., Devaux, B., Radolf, J. D., Klimpel, G. R., Godowski, P., and Zychlinsky, A. (1999) Cell activation and apoptosis by bacterial lipoproteins through Toll-like receptor-2. *Science 285*, 736−739.
(19) Krieg, A. M., Yi, A. K., Matson, S., Waldschmidt, T. J., Bishop, G. A., Teasdale, R., Koretzky, G. A., and Klinman, D. M. (1995) CpG motifs in bacterial DNA trigger direct B-cell activation. *Nature 374*, 546−549.
(20) Chan, M., Hayashi, T., Mathewson, R. D., Nour, A., Hayashi, Y., Yao, S., Tawatao, R. I., Crain, B., Tsigelny, I. F., Kouznetsova, V. L., Messer, K., Pu, M., Corr, M., Carson, D. A., and Cottam, H. B. (2013) Identification of substituted pyrimido[5,4-b] indoles as selective toll-like receptor 4 ligands. *J. Med. Chem. 56*, 4206−4223.
(21) Chan, M., Kakitsubata, Y., Hayashi, T., Ahmadi, A., Yao, S., Shukla, N. M., Oyama, S. Y., Baba, A., Nguyen, B., Corr, M., Suda, Y., Carson, D. A., Cottam, H. B., and Wakao, M. (2017) Structure-Activity Relationship Studies of Pyrimido[5,4-b] indoles as Selective Toll-Like Receptor 4 Ligands. *J. Med. Chem. 60*, 9142−9161.
(22) Shukla, N. M., Malladi, S. S., Mutz, C. A., Balakrishna, R., and David, S. A. (2010) Structure-activity relationships in human toll-like receptor 7-active imidazoquinoline analogues. *J. Med. Chem. 53*, 4450−4465.
(23) Shukla, N. M., Mutz, C. A., Malladi, S. S., Warshakoon, H. J., Balakrishna, R., and David, S. A. (2012) Toll-like receptor (TLR)-7 and −8 modulatory activities of dimeric imidazoquinolines. *J. Med. Chem. 55*, 1106−1116.
(24) Hamley, I. W., Kirkham, S., Dehsorkhi, A., Castelletto, V., Reza, M., and Ruokolainen, J. (2014) Toll-like receptor agonist lipopeptides self-assemble into distinct nanostructures. *Chem. Commun. 50*, 15948−51.
(25) Takeda, K., and Akira, S. (2004) TLR signaling pathways. *Semin. Immunol. 16*, 3−9.
(26) Napolitani, G., Rinaldi, A., Bertoni, F., Sallusto, F., and Lanzavecchia, A. (2005) Selected Toll-like receptor agonist combinations synergistically trigger a T helper type 1 -polarizing program in dendritic cells. *Nat. Immunol. 6*, 769−776.
(27) Trinchieri, G., and Sher, A. (2007) Cooperation of Toll-like receptor signals in innate immune defence. *Nat. Rev. Immunol. 7*, 179−190.

(28) Liu, Q., and Ding, J. L. (2016) The molecular mechanisms of TLR-signaling cooperation in cytokine regulation. Immunol. *Immunol. Cell Biol. 94*, 538−42.
(29) Karin, M., and Ben-Neriah, Y. (2000) Phosphorylation Meets Ubiquitination: The Control of NF-κB Activity. *Annu. Rev. Immunol. 18*, 621−663.
(30) Ernst, O., Vayttaden, S. J., and Fraser, I. D. C. (2018) Measurement of NF-κB activation in TLR-activated macrophages. *Methods Mol. Biol. 1714*, 67−78.

https://dx.doi.org/10.1021/acschembio.0c00924
ACS Chem. Biol. 2021, 16, 380−388